

# Frmd7 expression in developing mouse brain

J Self<sup>1,2,4,5</sup>, HM Haitchi<sup>3,5</sup>, H Griffiths<sup>2</sup>, ST Holgate<sup>3</sup>, DE Davies<sup>3</sup> and A Lotery<sup>1,4,2</sup>

LABORATORY STUDY

## Abstract

**Aims** Mutations in the FERM domain containing 7 (*FRMD7*) genes are known to cause a significant number of cases of congenital idiopathic nystagmus (CIN). Only limited expression data exist suggesting low levels of expression in all tissues. In this study, we assess the expression profile of the murine homologue of *FRMD7* (*Frmd7*) in tissue from three murine organs during development.

**Methods** cDNA was extracted from heart, lung, and brain tissues of MF-1 mice at 12 developmental time points, embryonic days 11–19, postnatal days 1 and 8, and from adult mice. Relative expression of *Frmd7* mRNA was calculated using quantitative real-time PCR techniques with two normalising genes (*Gapdh* and *Actb*).

**Results** Expression of *Frmd7* was low in all tissues consistent with earlier reports. In heart and lung tissues, expression remained very low with an increase only in adult samples. In brain tissue, expression levels were higher at all time points with a significant increase at embryonic day 18, with no gender-specific influence on *Frmd7* expression.

**Conclusions** *Frmd7* is expressed at low levels in all tissues studied suggesting a role in many tissue types. However, higher overall expression and a sharp increase at ED18 in the murine brain suggest a different role in this tissue.

Earlier studies have shown that genes expressed in the murine brain during development exhibit temporal functional clustering. The temporal pattern of *Frmd7* expression found in this study mirrors that of genes involved in synapse formation/function, and genes related to axon growth/guidance. This suggests a role for *Frmd7* in these processes and should direct further expression studies.

*Eye* (2010) 24, 165–169; doi:10.1038/eye.2009.44; published online 6 March 2009

**Keywords:** nystagmus; expression; *Frmd7*; developing mouse brain

## Introduction

In November 2006, Tarpey *et al*<sup>1</sup> identified 22 nystagmus-causing mutations in the FERM domain containing 7 (*FRMD7*) genes, which resides within the Xq26-q27 interval. Since then, Self *et al*<sup>2</sup> and a number of other groups have confirmed that mutations in this gene are an important cause of congenital idiopathic nystagmus (CIN). At present, the function of this gene is unknown and its expression profile poorly understood. There is some evidence that the mRNA for *FRMD7* is present at low levels in most tissues, and possibly the greatest in the kidney and testis (<http://symatlas.gnf.org>). Using RT-PCR, Tarpey *et al*<sup>1</sup> detected *FRMD7* mRNA expression in human adult kidney, liver, pancreas, and at lower levels in heart and brain.<sup>1</sup> However, in human foetal tissue, they found the transcript only in kidney. Using *in situ* hybridisation applied to human embryonic brain at day 56 postovulation, there was *FRMD7* expression in the ventricular layer of the forebrain, midbrain, cerebellar primordium, spinal cord, and developing neural retina. At day 37, postovulation embryos, expression was restricted to the mid- and hindbrain, regions known to be involved in motor control of eye movement.<sup>1</sup> No temporal profile or further expression study has been published in any species to date.

It has been postulated that the *FRMD7* gene is likely to be involved in neuronal development.<sup>1–3</sup> It is also known that gaining an understanding of the spatial and temporal expressions of such genes can provide some insight into complex self-organizing processes, such as mammalian central nervous system development.<sup>4</sup> Here, we describe a detailed temporal expression study of *Frmd7* in the developing brain, lung, and heart in mice.

<sup>1</sup>Southampton Eye Unit, Southampton General Hospital, UK

<sup>2</sup>Clinical Neurosciences Division, School of Medicine, University of Southampton, UK

<sup>3</sup>Roger Brooke Laboratory, Division of Infection, Inflammation and Repair, School of Medicine, University of Southampton, UK

<sup>4</sup>Department of Neurology, Southampton General Hospital, UK

<sup>5</sup>These authors contributed equally to this work

Correspondence: A Lotery, Division of Clinical Neurosciences, Southampton General Hospital, Mail point 806, South Lab and Path Block, SO16 6YD, Tel: +2380795049; Fax: +2380794542. E-mail: a.j.lotery@southampton.ac.uk

Received: 16 July 2008  
Accepted in revised form: 6 February 2009  
Published online: 6 March 2009

Commercial interests: None

## Materials and methods

Specific pathogen-free 6-week-old outbred MF-1 mice (obtained from Harlan UK Ltd, Bicester, UK) were time-mated by the detection of a vaginal plug. This day was taken as embryonic day (ED) 0. Pregnant mice between ED10 and 20, newborn and juvenile mice were killed using a schedule 1 method (cervical dislocation). Gravid uteri were removed under sterile conditions, and embryos were killed according to schedule 1 method (neural tube dissection and cervical dislocation). Maternal adult, embryonic and postpartum lungs, hearts, and brains were dissected in a laminar flow hood. Embryos were dissected under a dissecting microscope (LEICA WILD M3Z, Wetzlar, Germany). The dissected lungs, hearts, and brains were then homogenised using a Hybaid RiboLyser Cell Disrupter (Thermo Life Sciences, Hybaid, UK) at speed settings 6.0s and for 40s in TRIzol (Invitrogen, Paisley, UK) and RNA extracted according to the TRIzol protocol. Developmental time points were represented by two animals from two mothers. Therefore, two independent samples were obtained from heart, brain, and lung for ED11–19 from adult female mice, and from the 1- and 8-day postdelivery (PD) pups.

RNA was extracted using TRIzol reagent, and samples were treated with DNase (Ambion, Austin, TX, USA) according to the manufacturer's instructions to remove trace contamination by genomic DNA. In all, 1 µg total RNA was reverse transcribed using reverse transcription kits (PrimerDesign Ltd, Southampton, UK) according to the manufacturers' instructions with the addition of both Oligo dT and random nonamer primers to maximise transcription. cDNA was diluted 1:10 in RNA/DNAase-free water and stored before use at -20°C.

The ubiquitously expressed gene *Eif2s3y*, located in a non-recombining region of the Y chromosome, is only expressed in male mouse tissues including the developing brain.<sup>5</sup> Quantitative real-time PCR (RT-qPCR) amplification and melt-curve analysis for *Eif2s3y* were used to determine male and female gender in cDNA samples from mouse brain, heart, and lung tissues.

### RT-qPCR protocol

RT-qPCR was performed to assess the relative abundance of murine *Frmd7* mRNA compared with two housekeeping genes: Glyceraldehyde-3-phosphate dehydrogenase (*Gapdh*) and Beta-actin (*Actb*). Although accuracy of comparative expression analysis can be improved by using greater numbers of housekeeping genes, the greatest increase in efficacy has been shown to be in using greater than one reference gene.<sup>6</sup> The choice

of these two housekeeping genes was based on their earlier use in heart, lung, and brain tissues,<sup>7</sup> and shows that their abundance is high and similar in these tissues.<sup>6</sup> Furthermore, these two genes have been employed previously for murine brain studies by RT-PCR, and *Gapdh* has been shown to have an almost constant expression value from ED10-P0.<sup>8</sup>

RT-qPCR was carried out using a custom-made RT-PCR assay for use with SYBRgreen chemistry (PrimerDesign Ltd) in a RT thermocycler Rotor-Gene 6000 real time thermo-analyser (Corbett Life Science, Brisbane, Australia). PCR reactions were performed according to the manufacturer's instructions for 45 cycles using the kit reagents, which included a chemical hot-start Taq polymerase. The primer sequences for the *Frmd7* gene were sense primer: ATGCAAGGCT TTCTGGAAGAC and an antisense primer: CGGAAACTGGAACCTTGCTA with an amplification product of 111 nucleotides. For the control genes, commercially available primers were obtained (PrimerDesign Ltd), and these sequences are the intellectual property of PrimerDesign Ltd.

PCR reactions were performed in 100-well Gene-Discs (6001–012, Corbett Life Science) on the Rotor-Gene 6000 real time thermo-analyser (Corbett Life Science). The Rotor Gene run settings were according to the standard protocol suggested for custom qPCR assays by PrimerDesign. Briefly, the two-step amplification conditions were enzyme activation for 10 min at 95°C, followed by 45 cycles of 15 s denaturation at 95°C, 60 s annealing, and extension at 60°C; and fluorescence data collection at the end of the denaturation step. A high-resolution melt-curve analysis was also performed for each run with ramping from 60–95°C with fluorescence data collection at 0.5°C increments. Melt-curve analysis allowed the assessment of specific amplification product at the predicted melting temperature for the primer set described above. Each developmental time point was represented by two samples from separate animals, and all samples were run in duplicate with duplicate water controls (cDNA replaced by water) for each assay.

### Data analyses

By monitoring the fluorescence values of each sample, it was possible to determine the quantity of PCR product on a cycle-by-cycle basis. To account for differences in background fluorescence, the Rotorgene software automatically normalised the data. Once normalisation was complete, a threshold at which fluorescence data was analysed was set. This threshold was set at a level where the rate of amplification was greatest during the exponential phase. In this experiment, the same

normalised threshold fluorescence value was used in all runs and was set at a value of 0.12. The number of cycles taken for each sample to reach the threshold level is defined as the  $C_t$ -value (threshold cycle), and is taken as a measure of the abundance of cDNA target present.

Results were analysed using the 'comparative  $C_t$  method,' which is also known as the 'delta-delta  $C_t$  method.'<sup>9</sup> In this method, values for the gene of interest are calculated relative to the controls genes expression for each sample, and then different samples are compared with respect to the relative expression of the gene of interest. For the purpose of these experiments, heart, brain, and lung samples were analysed separately and calibrated to the earliest time point sample. This method of analysis relies on a consistently efficient PCR over a range of cDNA concentrations such that each increase of 1 in  $C_t$  value is equivalent to a halving of template cDNA. For each assay, we performed a standard curve analysis to assess the PCR efficiencies over a range of template concentrations. For a PCR efficiency that is close to 100%, an efficiency measure of close to 1, and an  $R^2$  (a measure of the % data conforming to the given efficiency value)  $\sim 0.99$  is expected. Validation of the delta-delta  $C_t$  methodology was also provided by Primerdesign Ltd. Each of these assays had been tested for PCR efficiency during production and validation, and all assays were guaranteed to have a PCR efficiency close to 100%. This means that for analysis of relative mRNA expression, 1  $C_t$  value is equivalent to a onefold difference in copy number and the delta-delta  $C_t$  method of analysis is appropriate and valid.<sup>10</sup>

We certify that all applicable institutional and governmental regulations concerning the ethical use of animals were followed during this study

## Results

Initial standard curve analysis was performed to assess the validity of the delta-delta  $C_t$  method for relative expression analysis. PCR efficiency close to 100% was shown for *Gapdh* ( $R^2 = 0.994$ , efficiency = 1.03), *Actb* ( $R^2 = 0.9947$ , efficiency = 1.05), and *Frm7* ( $R^2 = 0.99628$ , efficiency = 0.92).

*Frm7* mRNA was expressed at low levels (up to 14  $C_t$  values later than control genes) in all three tissues. In all runs, *Gapdh*, *Actb*, and *Frm7* water controls showed no amplification until later than at least three  $C_t$  values behind cDNA samples, and had low broad melts indicative of mispriming resulting in non-specific amplification curves at very late  $C_t$  values.

Expression values were calculated relative to the ED11 sample from heart tissue, and are shown in Figure 1.

RT-qPCR amplification and melt-curve analysis for *Eif2s3y* were used to determine male and female gender

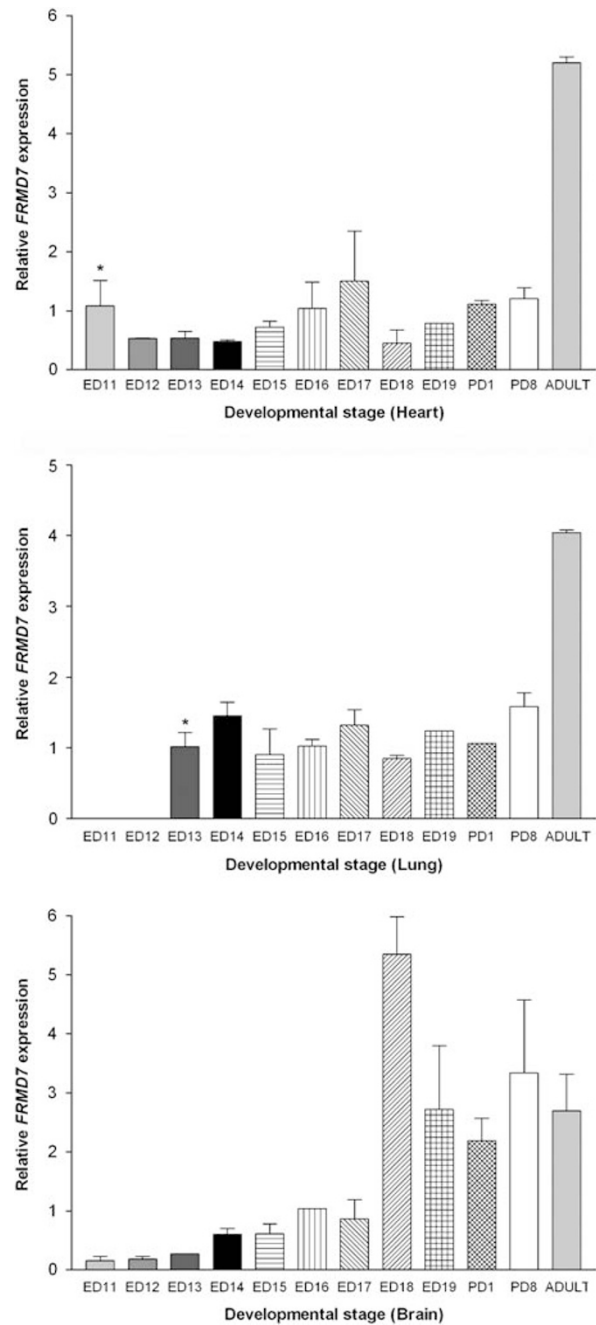


**Figure 1** Relative expression of *Frm7* in murine heart lung, and brain tissues during development. Expression data are shown compared with that of ED11 heart samples, and relative to the expression of the *Gapdh* and *Actb* housekeeping genes; \* = all samples were normalised to this sample. Error bars represent the SEM.

in cDNA samples from mouse brain, heart, and lung tissues. No significant difference of *Frm7* mRNA expression on ED18 between two male and two female brain, heart, and lung samples could be detected

suggesting no sex chromosome-specific influence on *Frmd7* expression.

## Discussion

Our results show that in murine heart and lung, *Frmd7* mRNA expression varied very little between ED11 and PD8. Interestingly, for both tissues, expression increased significantly in the adult samples following a similar pattern. In these tissues, overall expression of *Frmd7* was low during the developmental stages, and in most samples, the expression was at the limit of resolution for this technique. However, no significant increase in expression of *Frmd7* occurred during this critical period in murine development, and that overall expression in these tissues during development is very low and consistent with the previously reported 'low levels of expression in most tissues'.<sup>1</sup> *Frmd7* expression in murine brain samples were similarly low at early time points. However, as detailed previously, quantitative comparison between different tissues can be unreliable because of small differences in control gene expression, and so are not presented here. Interestingly, the overall pattern of expression in the brain tissue is noticeably different to that seen in the lung and heart tissues with a marked increase in the expression at ED18.

Genes expressed during murine development exhibit functional clustering in terms of temporal and spatial expression profiles during development.<sup>8,11</sup> In 2005, Matsuki *et al*<sup>8</sup> used an oligonucleotide-based microarray system to study the expression of 12 422 genes in mouse brain between ED11, ED15, ED18, and P0. They found significant differential expression in 1413 of these genes when normalised to the *ACTB* gene. These genes were then grouped into 15 clusters on the basis of cellular events involved in brain development and known/predicted gene function. Interestingly, only four of these clusters showed an overall temporal expression pattern similar to our *Frmd7* findings with low expression until a significant increase at ED18. These four clusters were carbohydrate, lipid, and amino-acid metabolism (CLAM); cell adhesion and recognition; neurotrophin, hormone, growth factor, and cytokine (NHGC); and neurotransmitter and ion channel genes (NT). This is an interesting finding as the CLAM genes supply molecular components required for active neurogenesis and histogenesis; NT supply molecular components for the formation of neuronal connectivity and circuits; and NHGC genes have a role in signalling for neural differentiation and survival.<sup>8</sup> All these processes are known to be occurring at this developmental stage, showing the efficacy of this clustering methodology and a possible role for *Frmd7* in these processes in murine

brain. This group subsequently selected 397 of these differentially expressed genes for which strong functional data were available. These genes were characterised into eight new clusters on the basis of their developmental function. Interestingly, the expression pattern of upregulation at ED18 or P0 was most strongly seen in two clusters. These clusters pertained to genes were involved in synapse formation and function (eg, genes coding GABA receptors and intracellular calcium channels) and axon growth and guidance-related genes (eg, *Sema4f* and *Cdh8*). Again, these results suggest a role for *Frmd7* in these processes in murine brain development. However, samples were taken from whole brain, and so there is no indication of which brain regions are expressing the gene at this time. Furthermore, earlier brain tissues used in this work (ED11–~ED14) will have included the developing optic vesicle (developing eye) and all samples of the developing primary visual cortex and connections. Therefore, no inference can be made from this study about which brain/eye structures are responsible for the peak in *Frmd7* expression at ED18 or the pathophysiology of CIN. Further expression on this gene would therefore be likely to include the expression analysis of various regions of the adult mouse brain.

It is important to note that in this study, detection of *Frmd7* expression was occurring at the limit of resolution for RT-qPCR. In many samples, the  $C_t$  difference between housekeeping genes and the *Frmd7* gene amplification curves was ~15 cycles. This corresponds to a difference in expression of 1:65536. At this very low level of expression, primer-dimer formation was occurred in poor samples, which were then necessarily excluded. Possibilities for improving results for such a low copy number gene include gene-specific RT-PCR and the use of fluorescent labelled probes for specific detection of the target transcript. Furthermore, relatively few samples were used per time point, and future work would benefit from a greater *N*-value, especially in light of the very low levels of expression detected. The final caveat to this study is that expression analysis was performed on murine samples with the possibility of differences to expression profiles in human tissues. For example, mice do not have fovea, and their eyes do not open until ~P10/11. Therefore, the visual systems of humans and mice are structurally different, and development occurs over differing timescales. However, the role of *Frmd7* in mice is likely to direct further study of this gene in humans, especially when a human FRMD7 antibody becomes available.

## Acknowledgements

We thank Angela Cree of the Gift of Sight Laboratory for technical and advisory support. Grant support was

provided by an MRC clinical research fellowship, a grant from the Nystagmus Network, and support from the AAIR (Asthma, Allergy, and Inflammation Research) charity.

## References

- 1 Tarpey P, Thomas S, Sarvananthan N, Mallya U, Lisgo S, Talbot CJ *et al*. Mutations in FRMD7, a newly identified member of the FERM family, cause X-linked idiopathic congenital nystagmus. *Nat Genet* 2006; **38**: 1242–1244.
- 2 Self JE, Shawkat F, Malpas CT, Thomas NS, Harris CM, Hodgkins PR *et al*. Allelic variation of the FRMD7 gene in congenital idiopathic nystagmus. *Arch Ophthalmol* 2007; **125**: 1255–1263.
- 3 Schorderet DF, Tiab L, Gaillard MC, Lorenz B, Klainguti G, Kerrison JB *et al*. Novel mutations in FRMD7 in X-linked congenital nystagmus. Mutation in brief no. 963. *Online Hum Mutat* 2007; **28**: 525.
- 4 Wen X, Fuhrman S, Michaels GS, Carr DB, Smith S, Barker JL *et al*. Large-scale temporal gene expression mapping of central nervous system development. *Proc Natl Acad Sci USA* 1998; **95**: 334–339.
- 5 Xu J, Burgoyne PS, Arnold AP. Sex differences in sex chromosome gene expression in mouse brain. *Hum Mol Genet* 2002; **11**: 1409–1419.
- 6 Vandesompele J, De PK, Pattyn F, Poppe B, Van RN, De PA *et al*. Accurate normalization of real-time quantitative RT-PCR data by geometric averaging of multiple internal control genes. *Genome Biol* 2002; **3**, RESEARCH0034.
- 7 Candenás L, Seda M, Noheda P, Buschmann H, Cintado CG, Martín JD *et al*. Molecular diversity of voltage-gated sodium channel alpha and beta subunit mRNAs in human tissues. *Eur J Pharmacol* 2006; **541**: 9–16.
- 8 Matsuki T, Hori G, Furuichi T. Gene expression profiling during the embryonic development of mouse brain using an oligonucleotide-based microarray system. *Brain Res Mol Brain Res* 2005; **136**: 231–254.
- 9 Schmittgen TD. Real-time quantitative PCR. *Methods* 2001; **25**: 383–385.
- 10 Bustin SA. Absolute quantification of mRNA using real-time reverse transcription polymerase chain reaction assays. *J Mol Endocrinol* 2000; **25**: 169–193.
- 11 Carotenuto P, Marino N, Bello AM, D'Angelo A, Di PU, Lombardi D *et al*. PRUNE and NM23-M1 expression in embryonic and adult mouse brain. *J Bioenerg Biomembr* 2006; **38**: 233–246.